SUPPLEMENTARY INFORMATION

Supplementary Figures

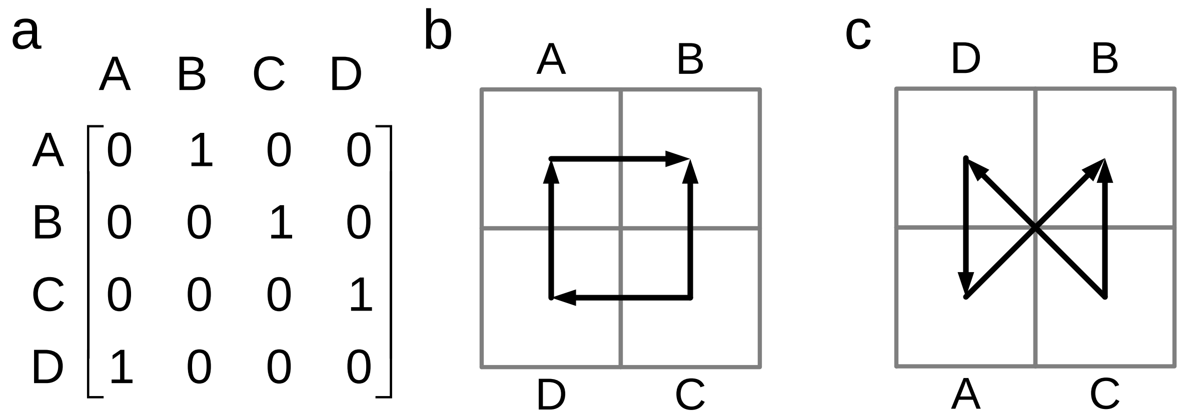

Supplementary Figure 1: **The importance of mobility directionality.** (a) an OD matrix between four locations: A, B, C and D. (b, c) Two different spatial distributions of the same OD matrix. Two schematic mobility distributions share the same topological structure (i.e., OD matrix), but different spatial layouts result in varying overall characteristics.

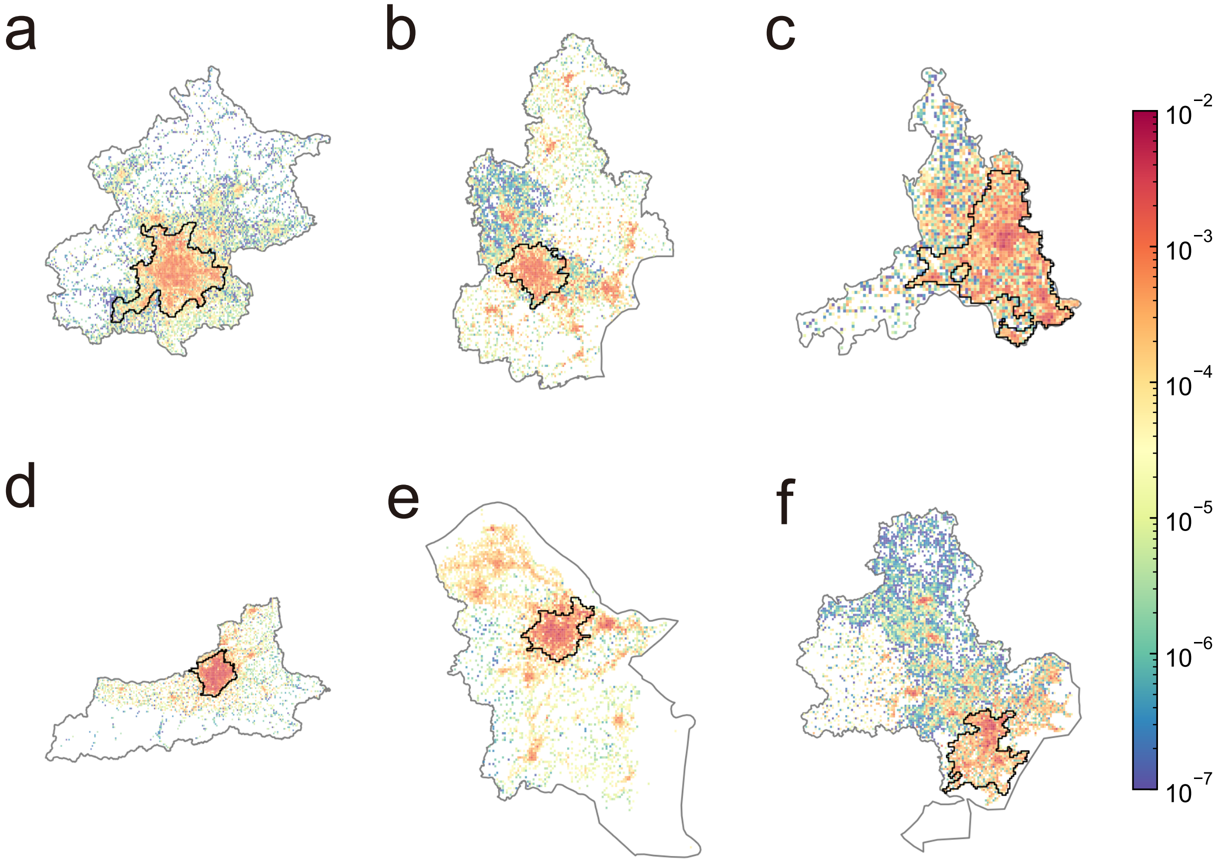

Supplementary Figure 2: **Comparison of the urban area and the outflow density distribution.** (a) Beijing, (b) Tianjin, (c) Foshan, (d) Xian, (e) Ningbo, (f) Quanzhou. The grey line is the administrative boundary and the black line is the boundary of the urban area extracted from the global human settlement dataset. Cells are colored according to their relative outflow (i.e., outflow adjusted by total outflow of all grids within the administrative boundary).

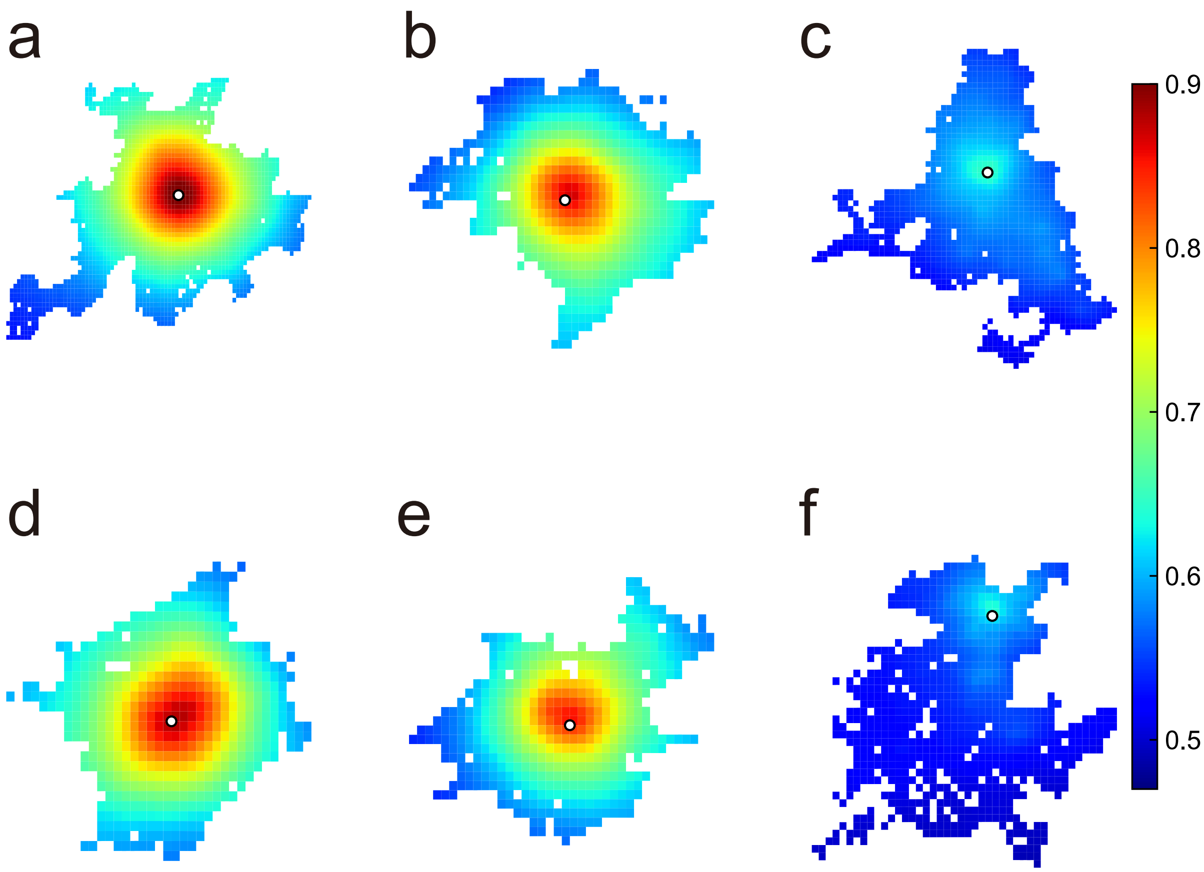

Supplementary Figure 3: **Urban mobility centripetality for each cell.** (a) Beijing, (b) Tianjin, (c) Foshan, (d) Xian, (e) Ningbo, (f) Quanzhou. Each cell is colored according to the centripetality Γ of urban mobility when this cell is regarded as the city center. The white dot represents the city center where Γ is maximum.

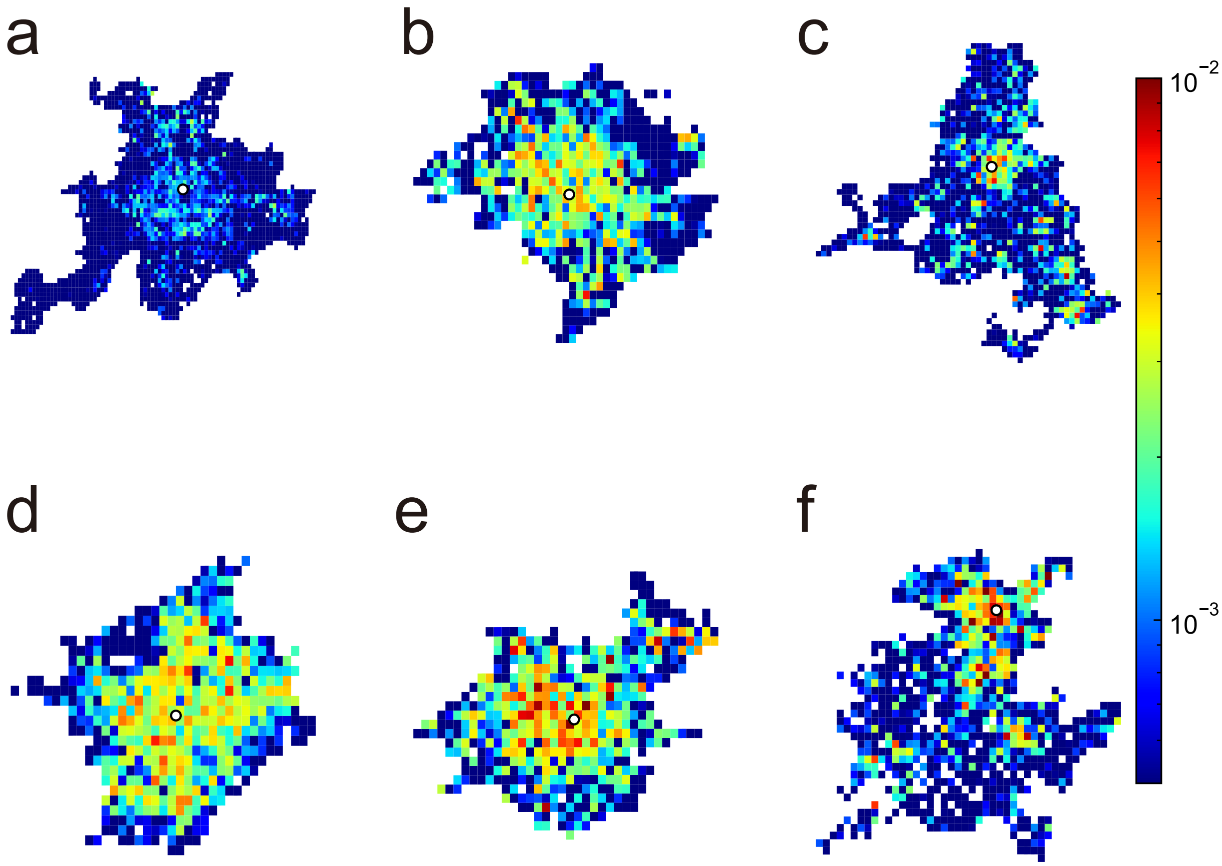

Supplementary Figure 4: **Examples of the identification of the city center.** (a) Beijing, (b) Tianjin, (c) Foshan, (d) Xian, (e) Ningbo, (f) Quanzhou. The white dot represents the city center. Cells are colored according to their relative outflow (i.e., outflow adjusted by total outflow of all grids within the urban area).

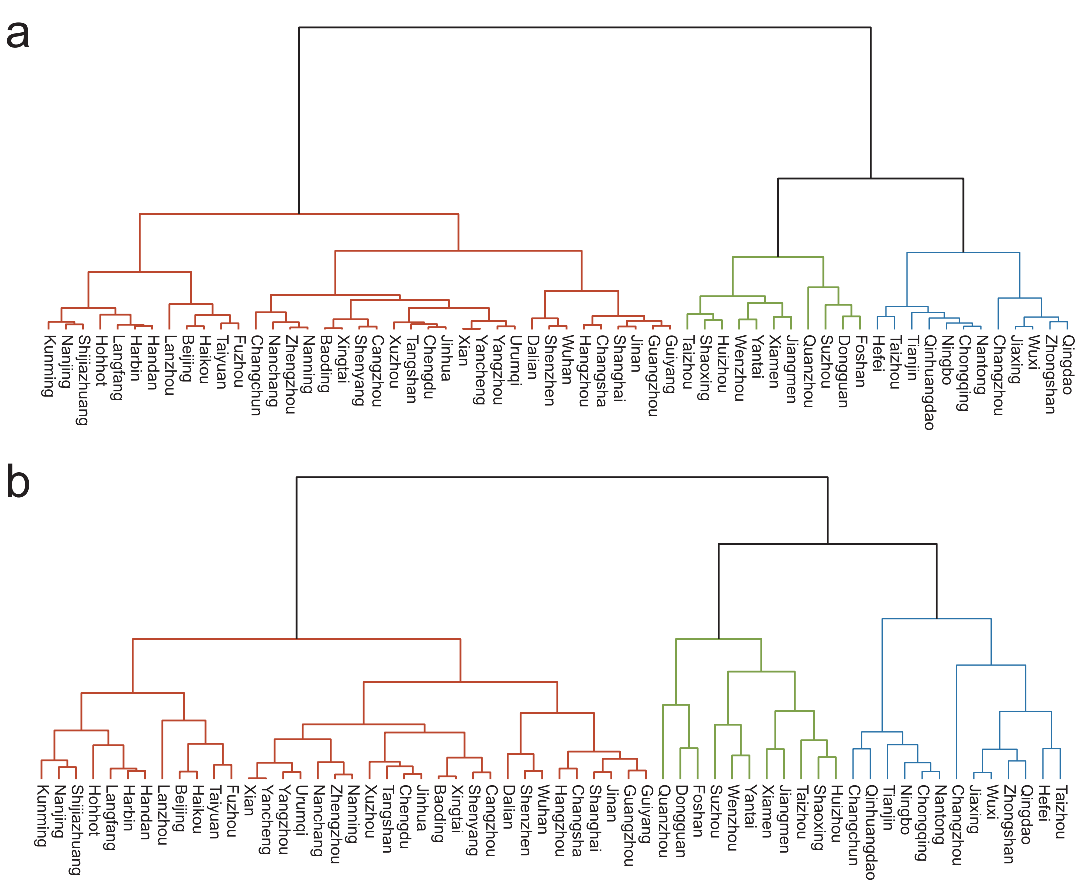

Supplementary Figure 5: **Classification of cites according to different approaches of hierarchical clustering.** Dendrogram resulting from the (a) Ward and (c) complete linkage approach, according to the anisotropy and centripetality of commuting flows. The colors illustrate a classification of three clusters.

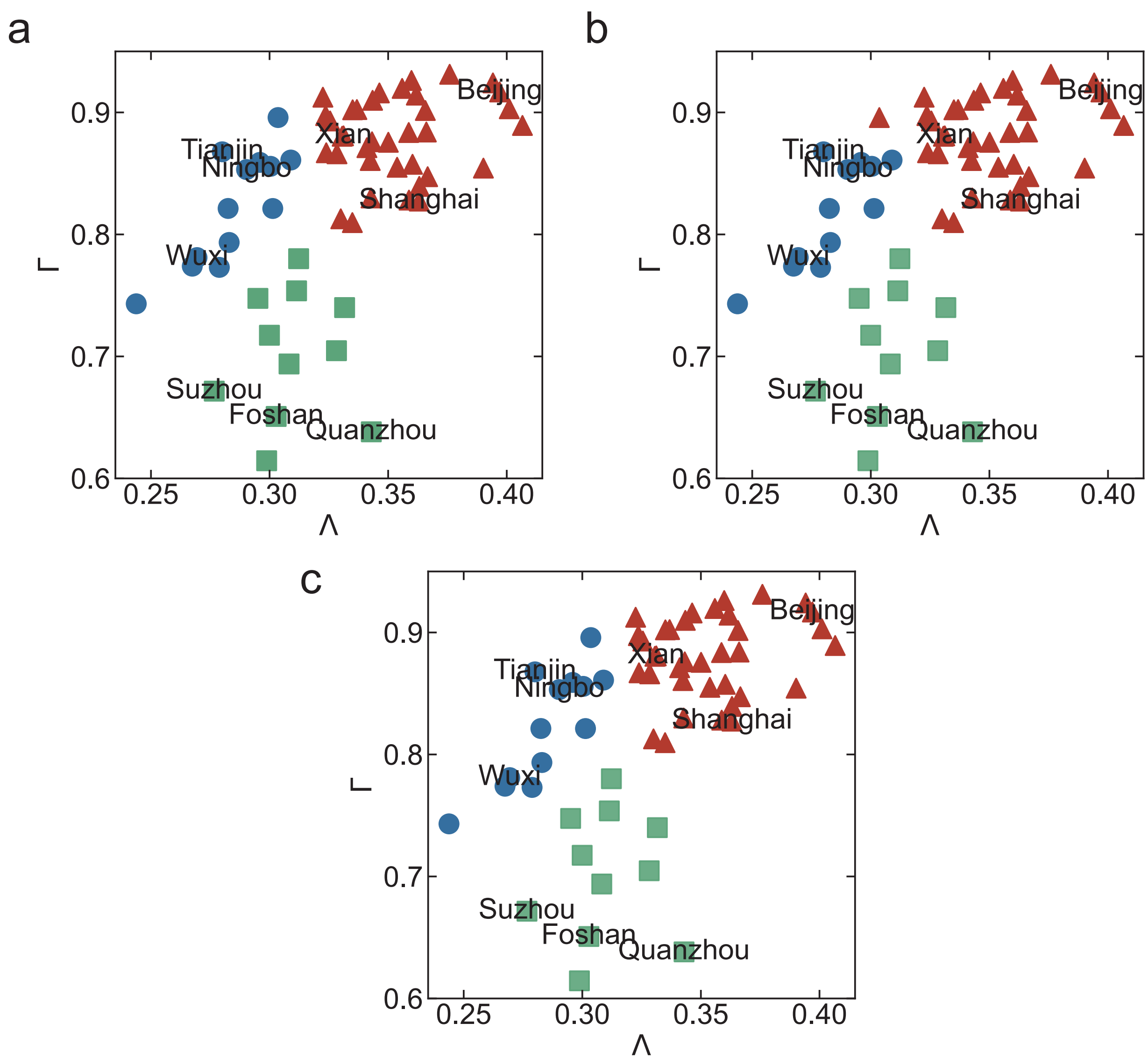

Supplementary Figure 6: **Three-clusters classification of cites.** The cities are divided into three types by their value of anisotropy and centripetality of commuting flows according to (a) average, (b) Ward and (c) complete linkage approach. The colors illustrate a classification of three clusters.

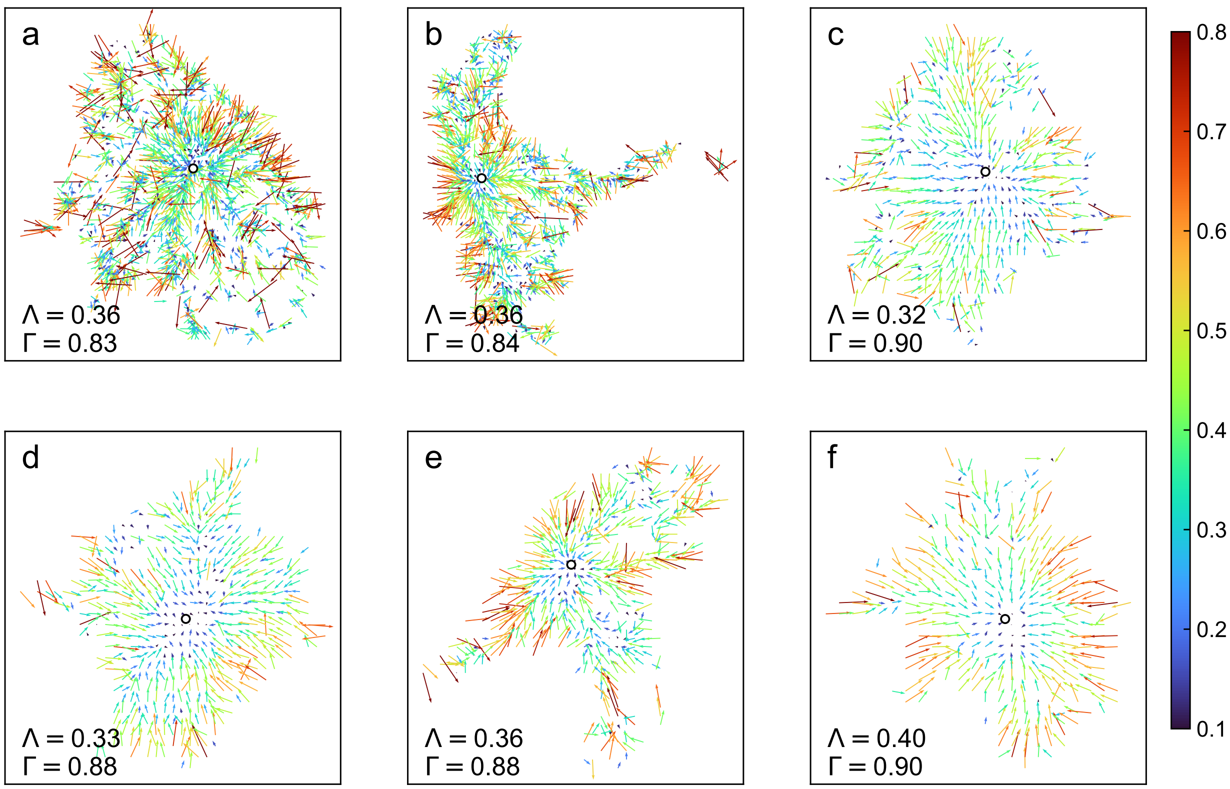

Supplementary Figure 7: **Representative samples of strong monocentric cities discussed in Fig. 2 of the main text.** Spatial distribution of PMVs for (a) Shanghai, (b) Guangzhou, (c) Zhengzhou, (d) Xian, (e) Nanjing and (f) Taiyuan.

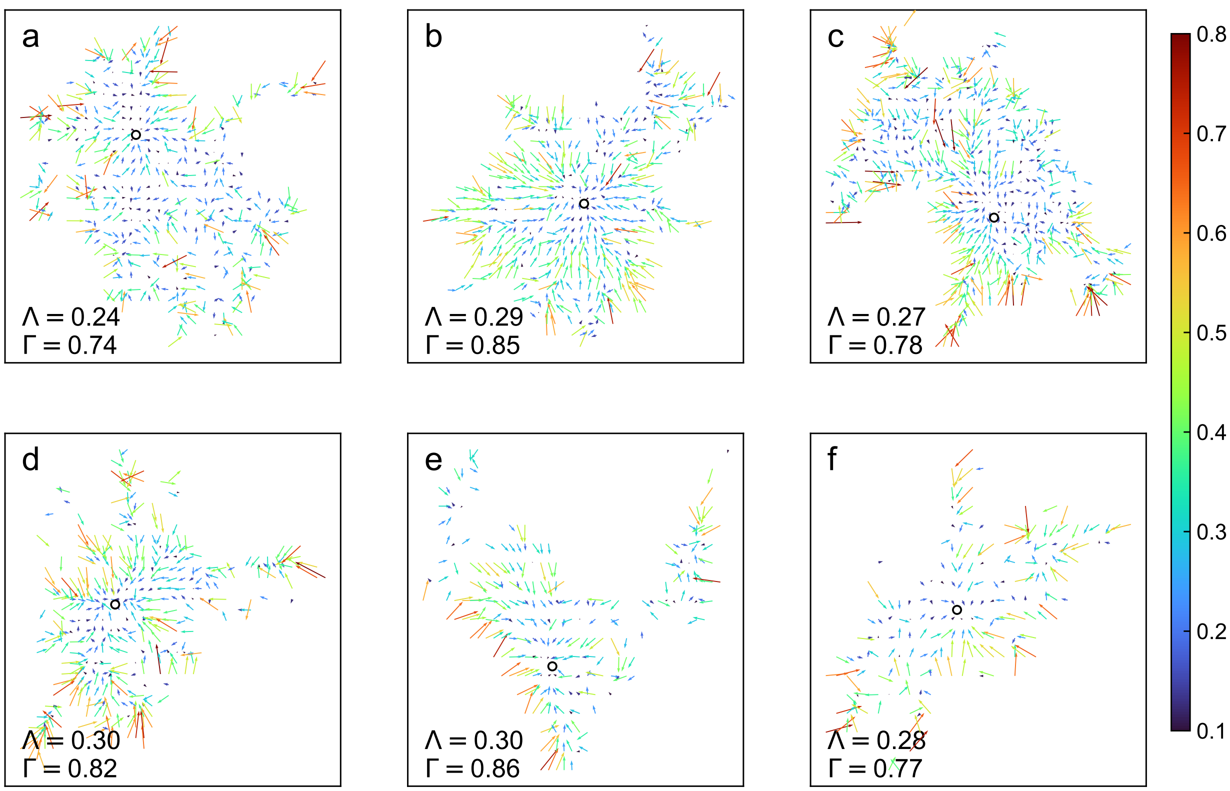

Supplementary Figure 8: **Representative samples of weak monocentric cities discussed in Fig. 2 of the main text.** Spatial distribution of PMVs for (a) Changzhou, (b) Ningbo, (c) Wuxi, (d) Hefei, (e) Nantong and (f) Zhongshan.

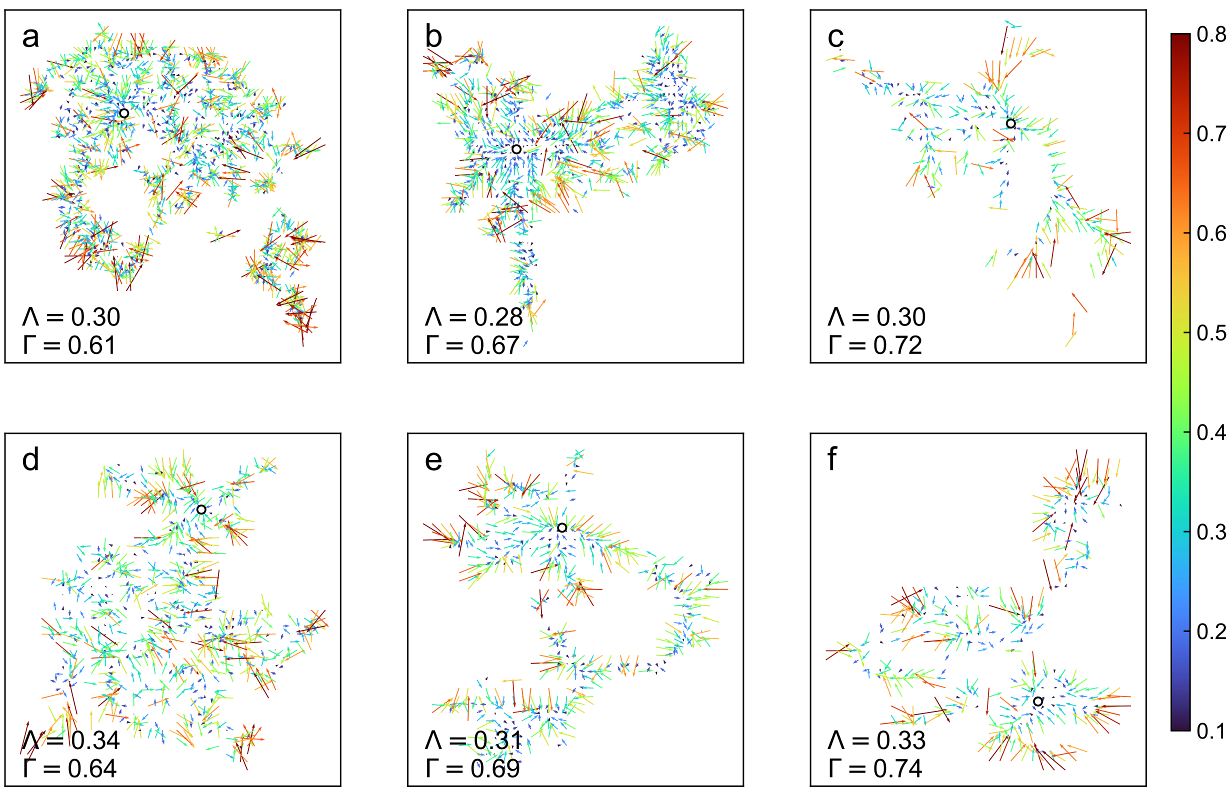

Supplementary Figure 9: **Representative samples of polycentric cities discussed in Fig. 2 of the main text.** Spatial distribution of PMVs for (a) Dongguan, (b) Suzhou, (c) Yantai, (d) Quanzhou, (e) Wenzhou and (f) Xiamen.

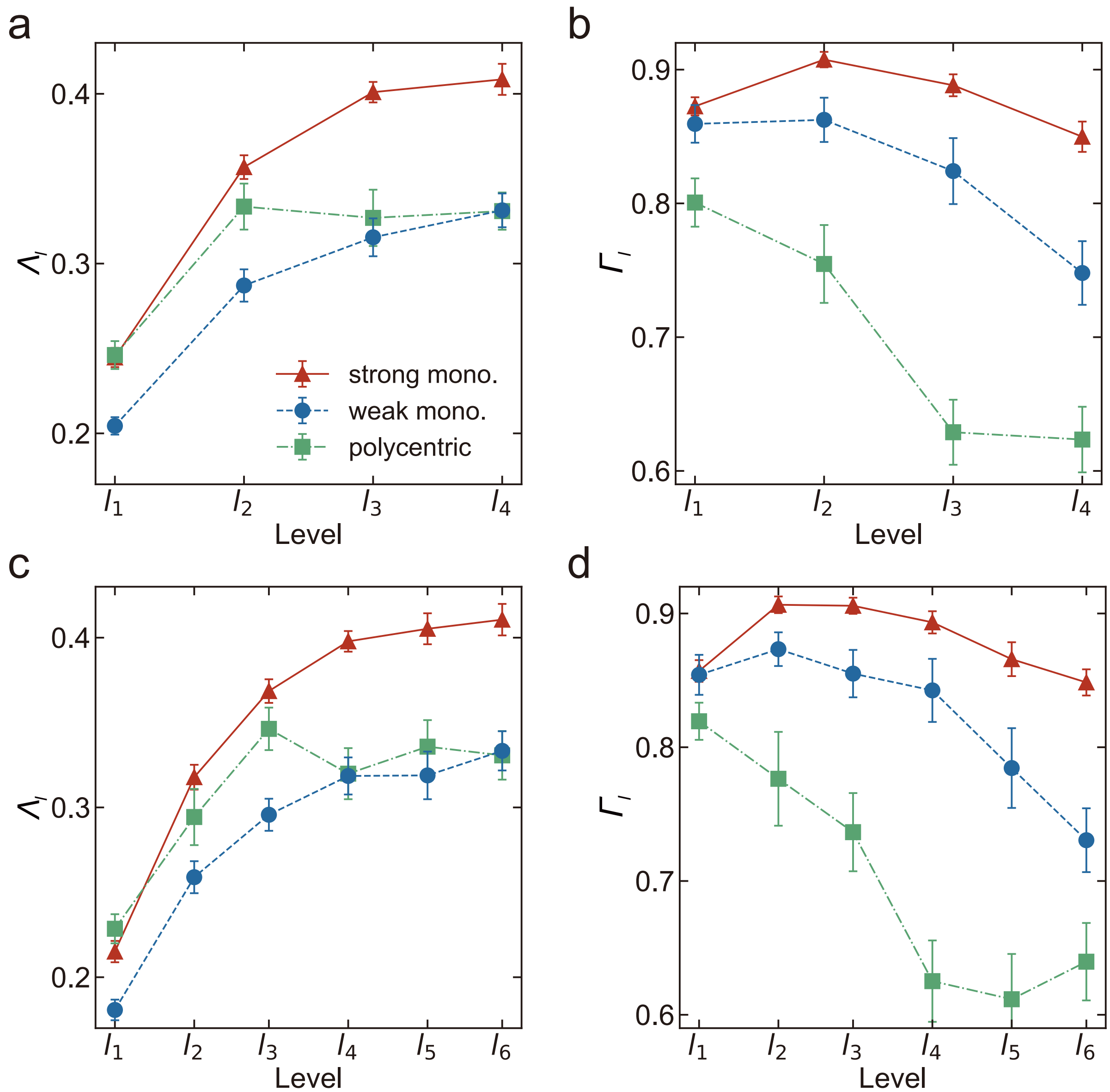

Supplementary Figure 10: **Robustness of the spatial distribution patterns of the anisotropy and centripetality against variations in the level l.** The (a) anisotropy and (b) centripetality of each spatial level for four spatial levels. The (c) anisotropy and (d) centripetality of each spatial level for six spatial levels. Error bars represent the standard error. Symbols and lines refer to various city types.

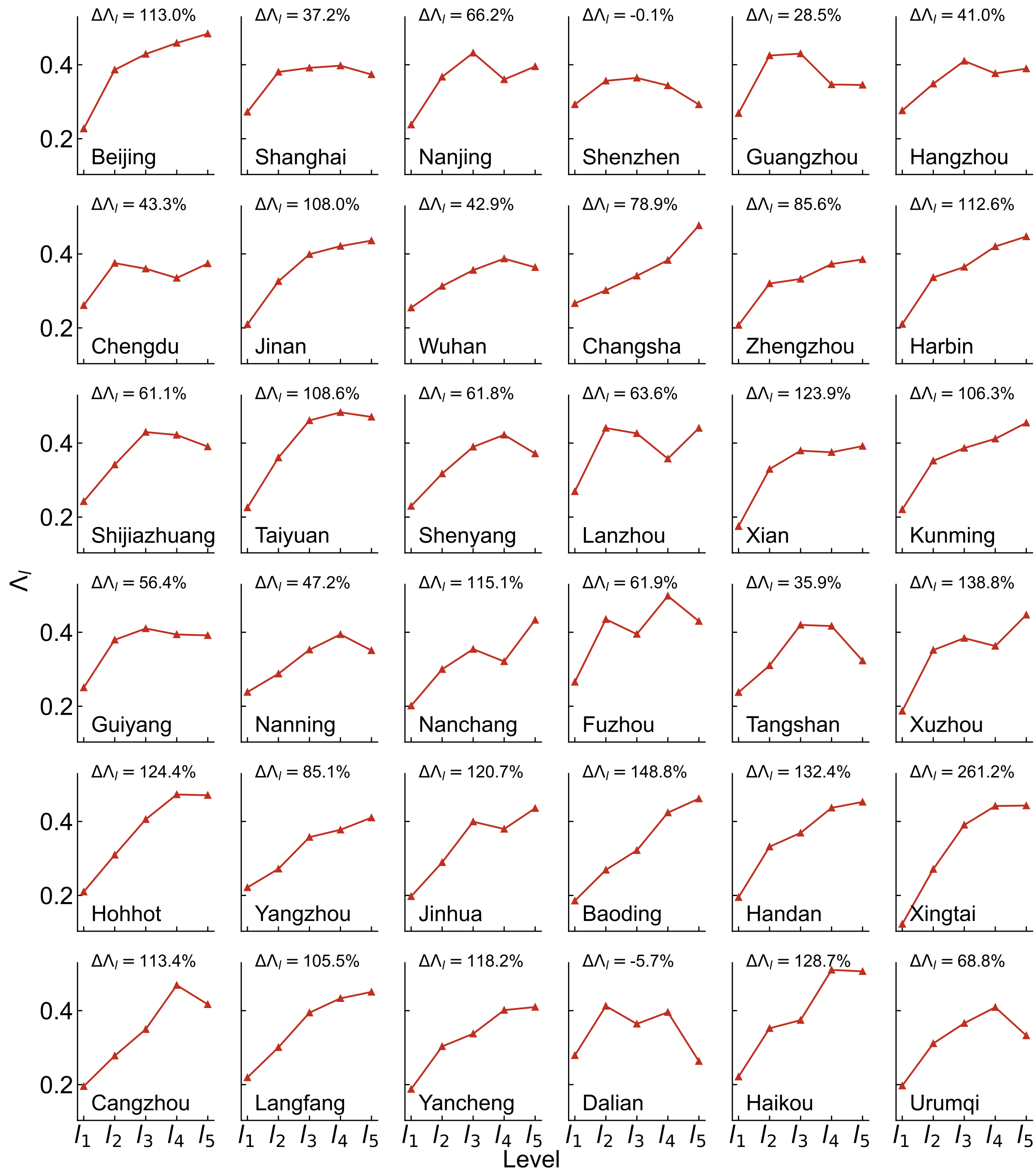

Supplementary Figure 11: **The trend of each level's anisotropy within individual city in strong monocentric type.** Markers in each panel present the anisotropy Λ_l for each level (distance to the city center). $\Delta\Lambda_l$ represents the increased ratio of anisotropy from level l_1 to level l_5. Overall, there is a noticeable increase in anisotropy Λ_l from level l_1 to level l_5 for most strong monocentric cities, excluding Shenzhen and Dalian, which exhibit irregular topologies compared to the others.

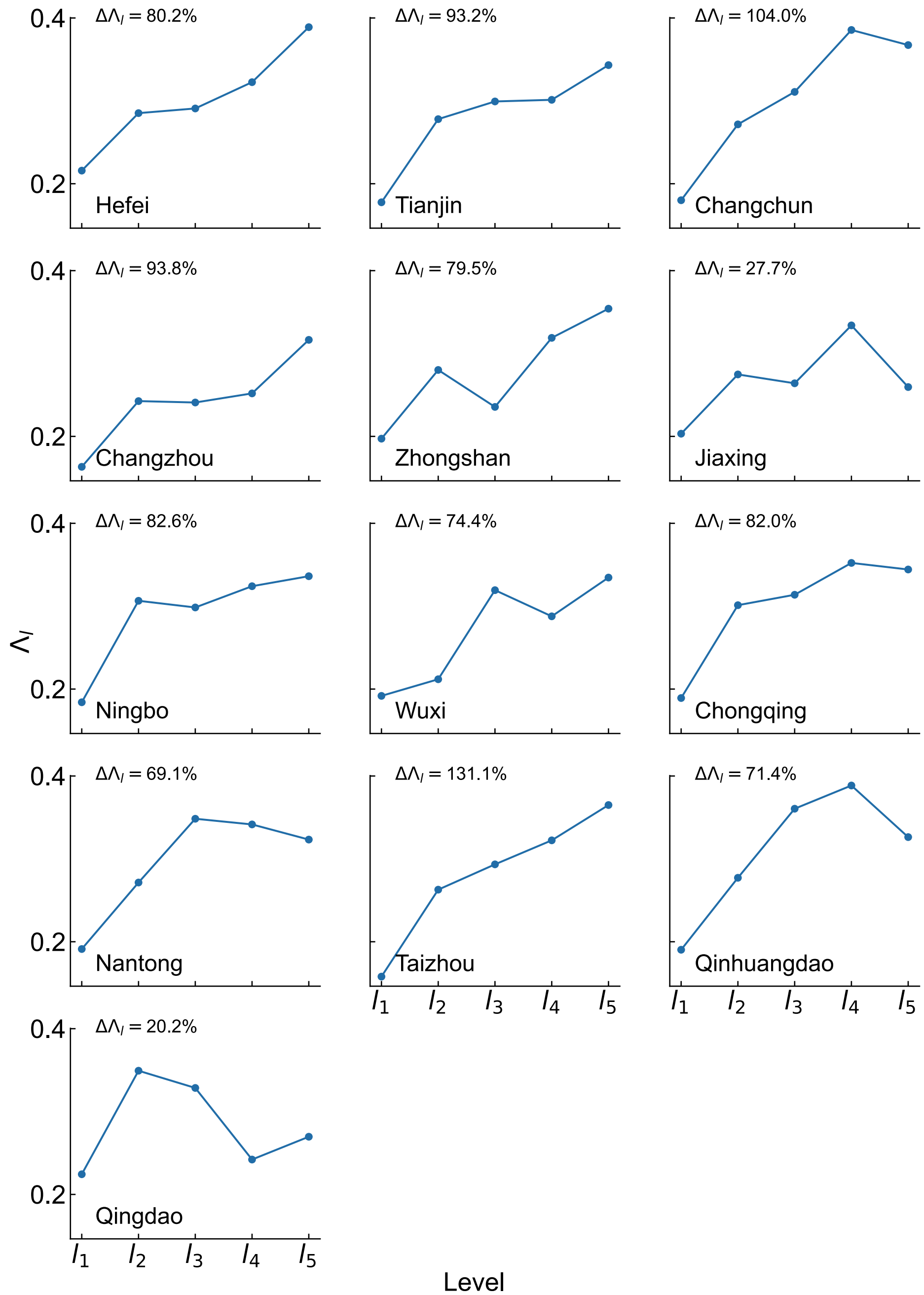

Supplementary Figure 12: **The trend of each level's anisotropy within individual city in weak monocentric type.** Markers in each panel present the anisotropy Λ_l for each level (distance to the city center). $\Delta\Lambda_l$ represents the increased ratio of anisotropy from level l_1 to level l_5. Overall, there is a noticeable increase in anisotropy Λ_l from level l_1 to level l_5 for most weak monocentric cities, excluding Qingdao, which exhibits irregular topology compared to the others.

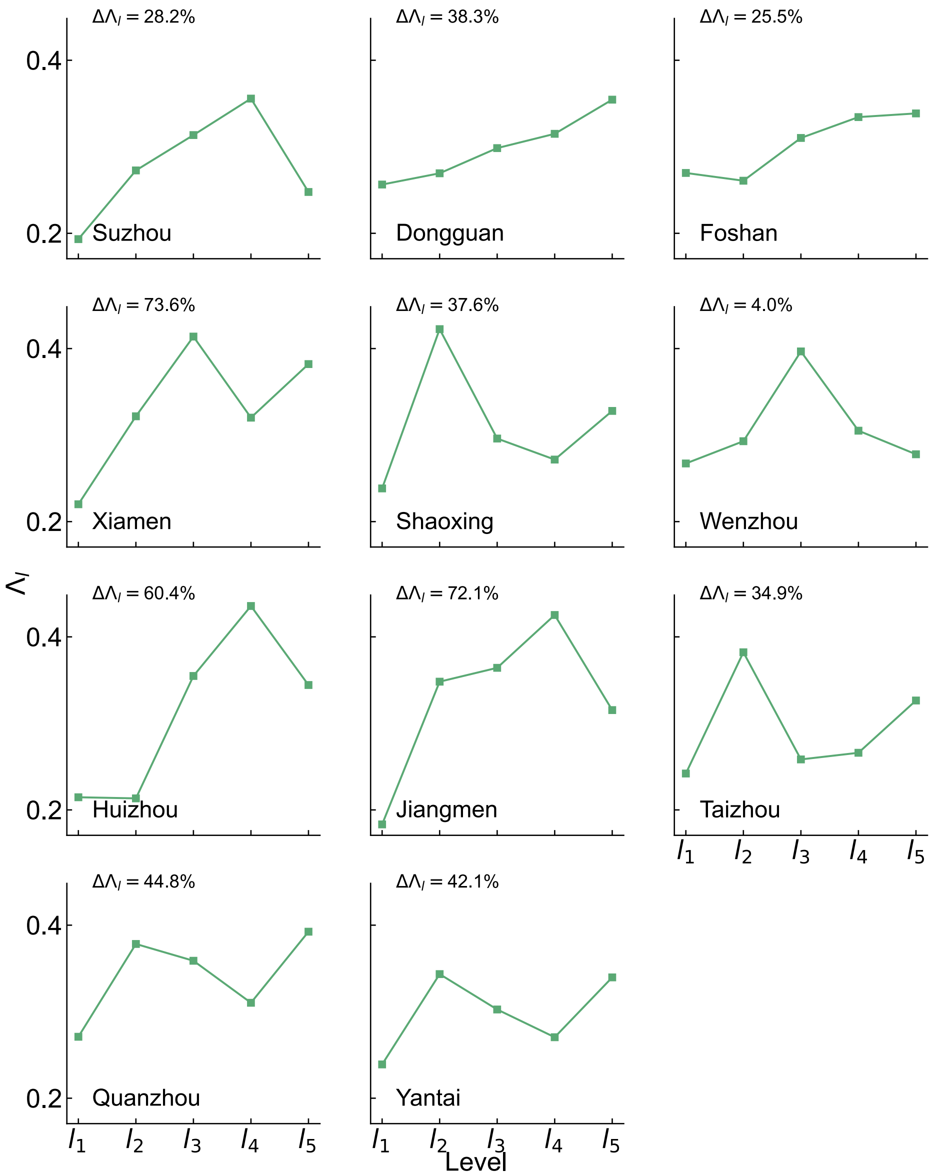

Supplementary Figure 13: **The trend of each level's anisotropy within individual city in polycentric type.** Markers in each panel present the anisotropy Λ_l for each level (distance to the city center). $\Delta\Lambda_l$ represents the increased ratio of anisotropy from level l_1 to level l_5. Overall, there is a noticeable increase in anisotropy Λ_l from level l_1 to level l_5.

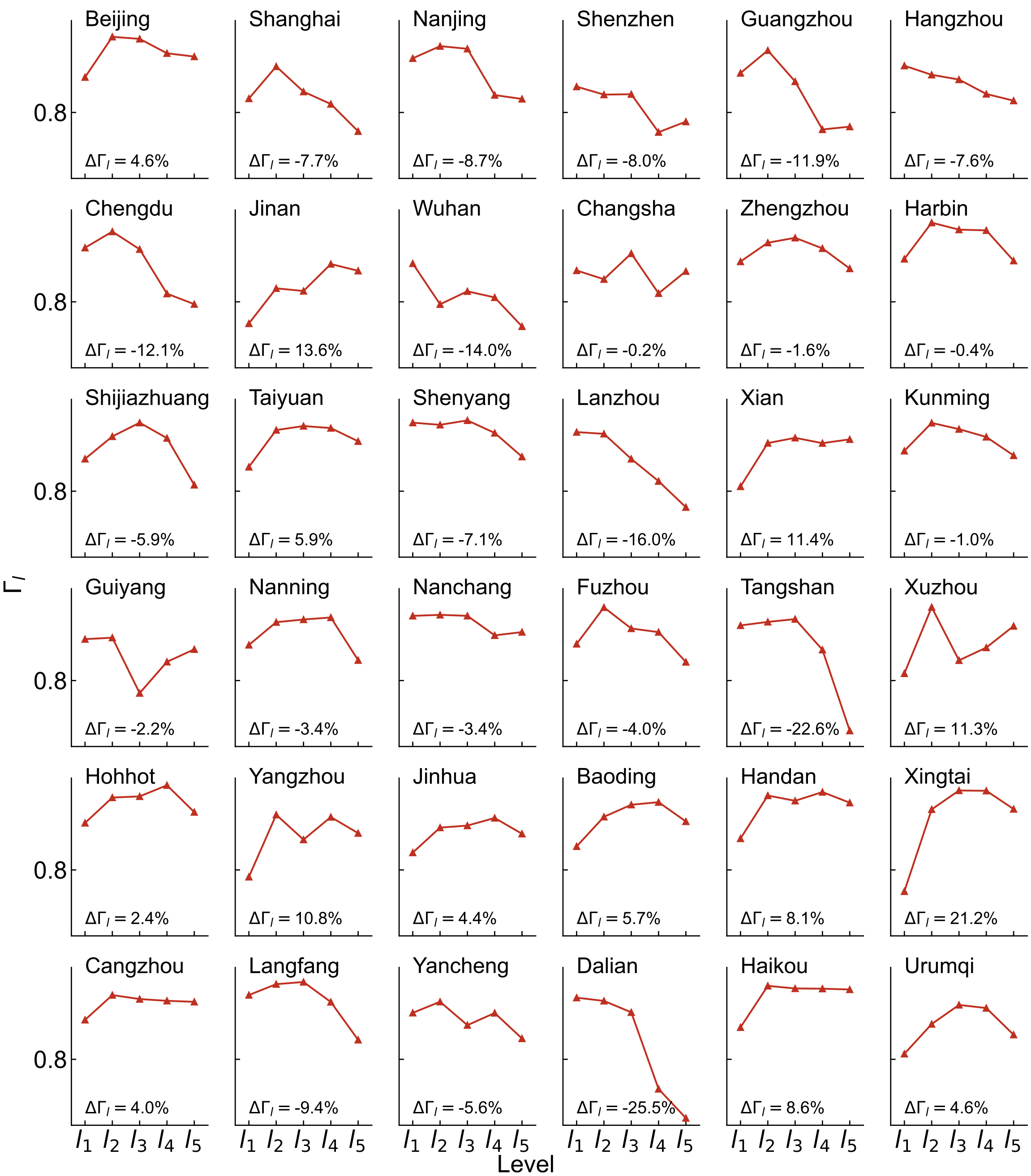

Supplementary Figure 14: **The trend of each level's centripetality within individual city in strong monocentric type.** Markers in each panel present the centripetality Γ_l for each level (distance to the city center). $\Delta\Gamma_l$ represents the decreased ratio of centripetality from level l_1 to level l_5. Overall, there is a noticeable decrease in centripetality Γ_l from level l_1 to level l_5 for most strong monocentric cities, except for some cities with exceptionally strong central attractivity, such as Beijing. However, the centripetality of these cities also begins to gradually weaken after level l_2 or l_3.

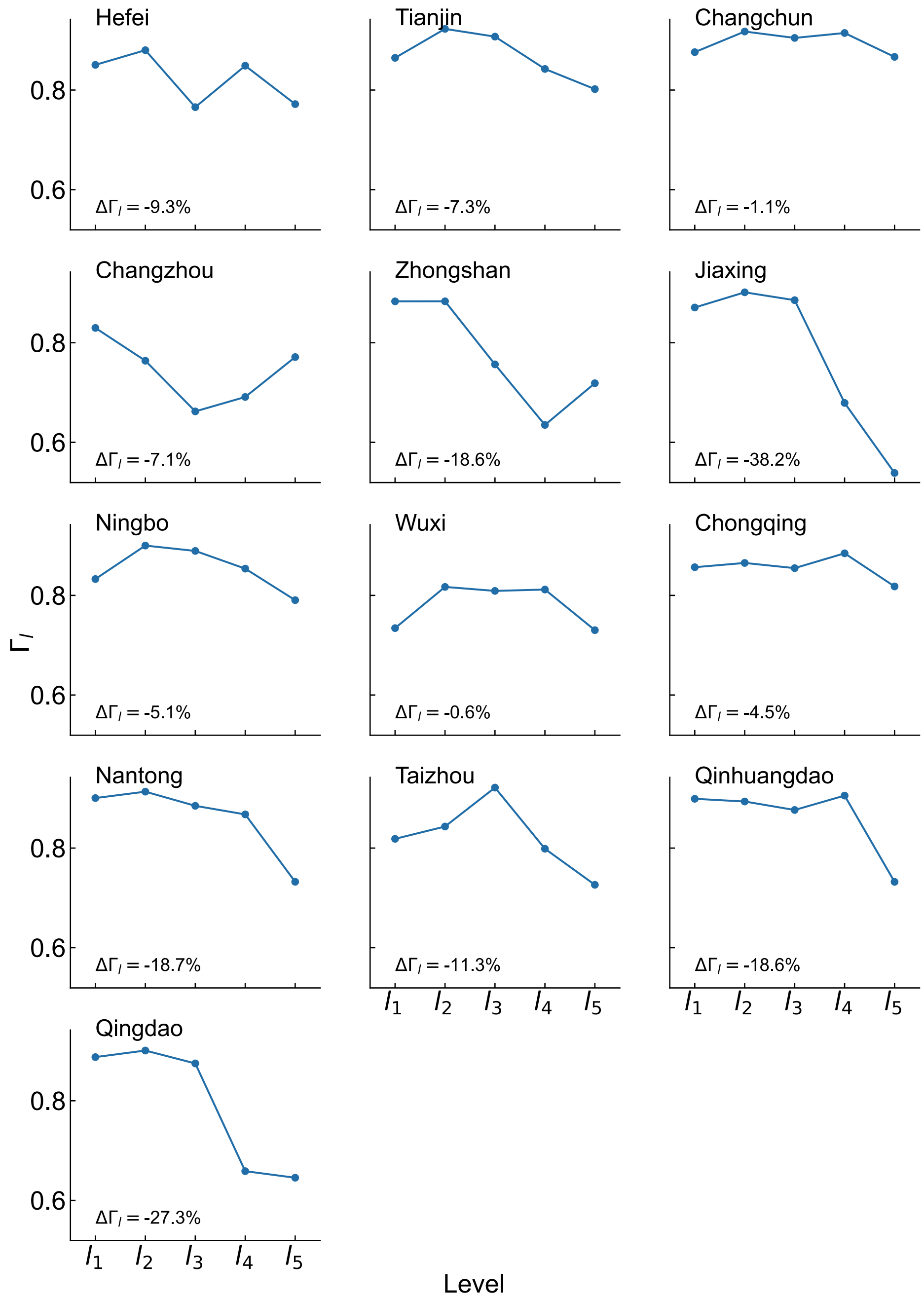

Supplementary Figure 15: **The trend of each level's centripetality within individual city in weak monocentric type.** Markers in each panel present the centripetality Γ_l for each level (distance to the city center). $\Delta\Gamma_l$ represents the decreased ratio of centripetality from level l_1 to level l_5. Overall, there is a noticeable decrease in centripetality Γ_l from level l_1 to level l_5.

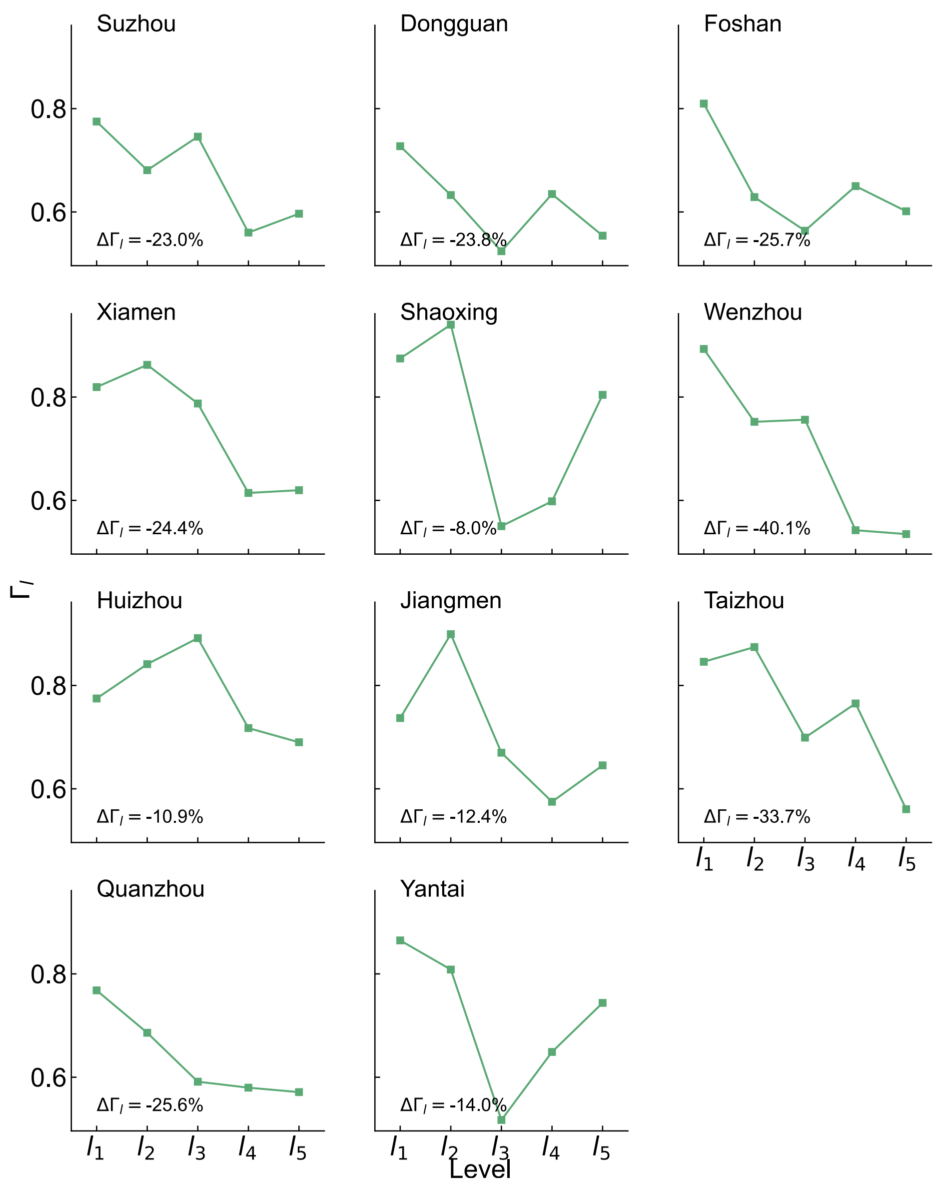

Supplementary Figure 16: **The trend of each level's centripetality within individual city in polycentric type.** Markers in each panel present the centripetality Γ_l for each level (distance to the city center). $\Delta\Gamma_l$ represents the decreased ratio of centripetality from level l_1 to level l_5. Overall, there is a noticeable decrease in centripetality Γ_l from level l_1 to level l_5.

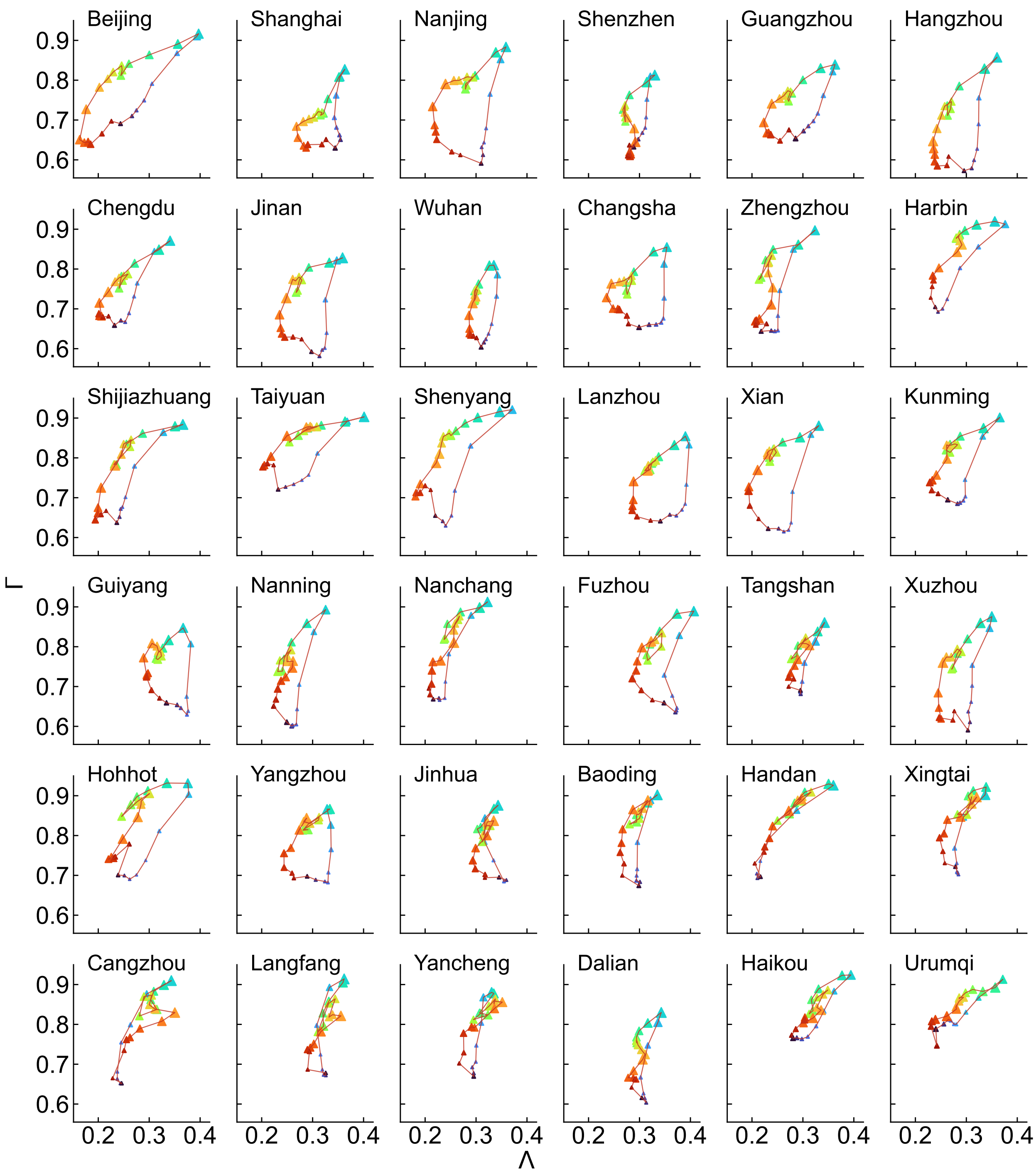

Supplementary Figure 17: **Hourly anisotropy and centripetality of urban mobility for each city in strong monocentric type.**

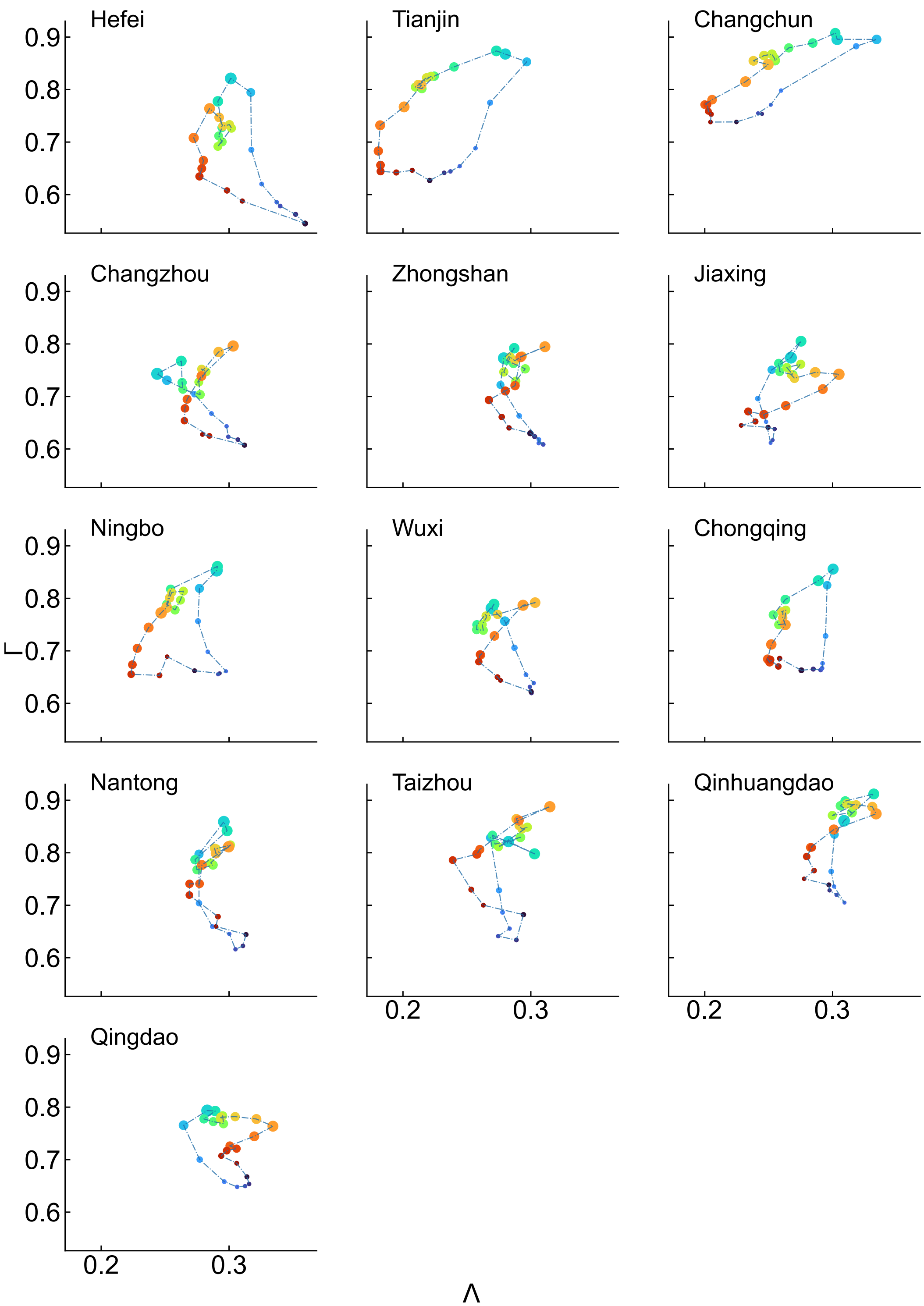

Supplementary Figure 18: **Hourly anisotropy and centripetality of urban mobility for each city in weak monocentric type.**

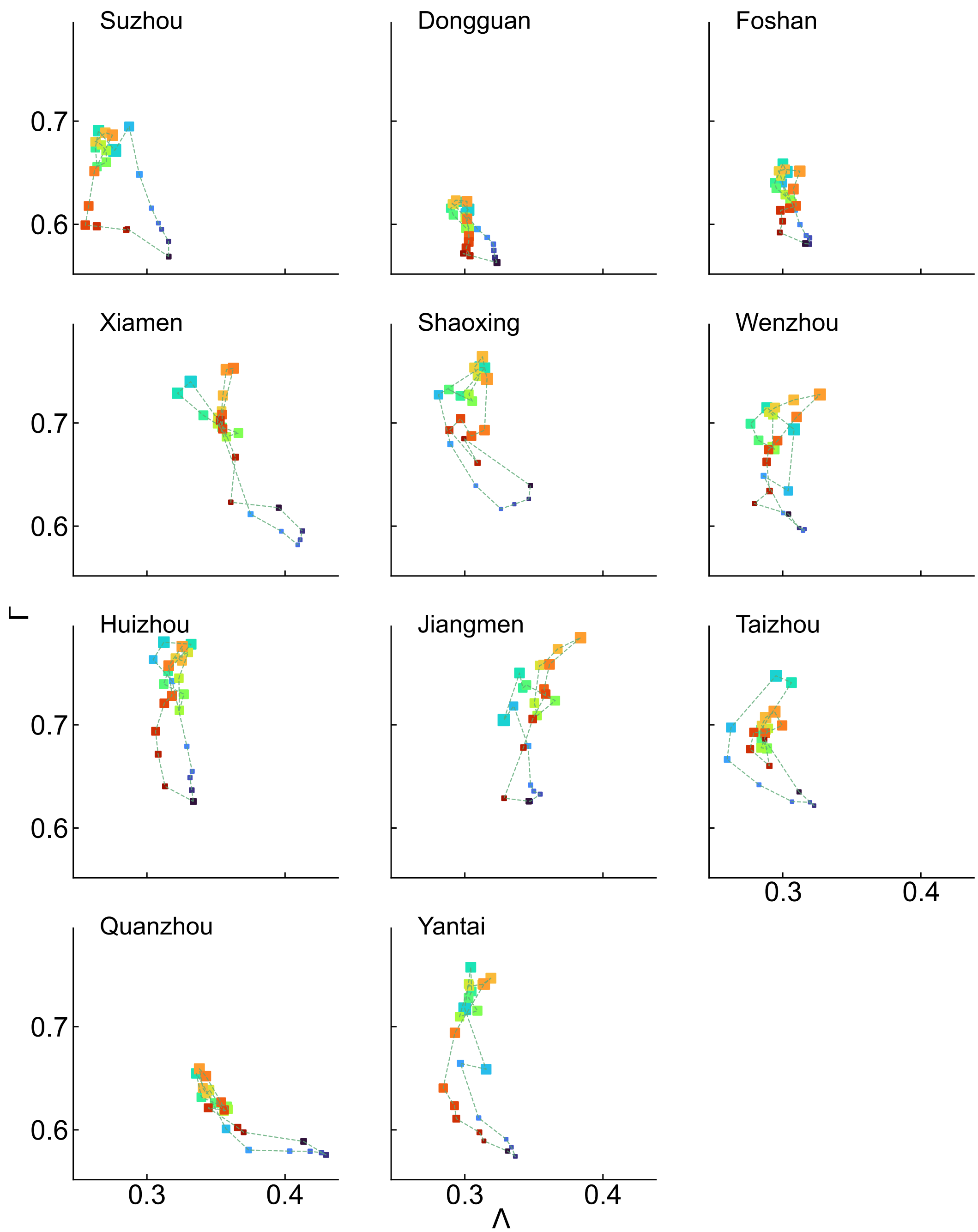

Supplementary Figure 19: **Hourly anisotropy and centripetality of urban mobility for each city in polycentric type.**

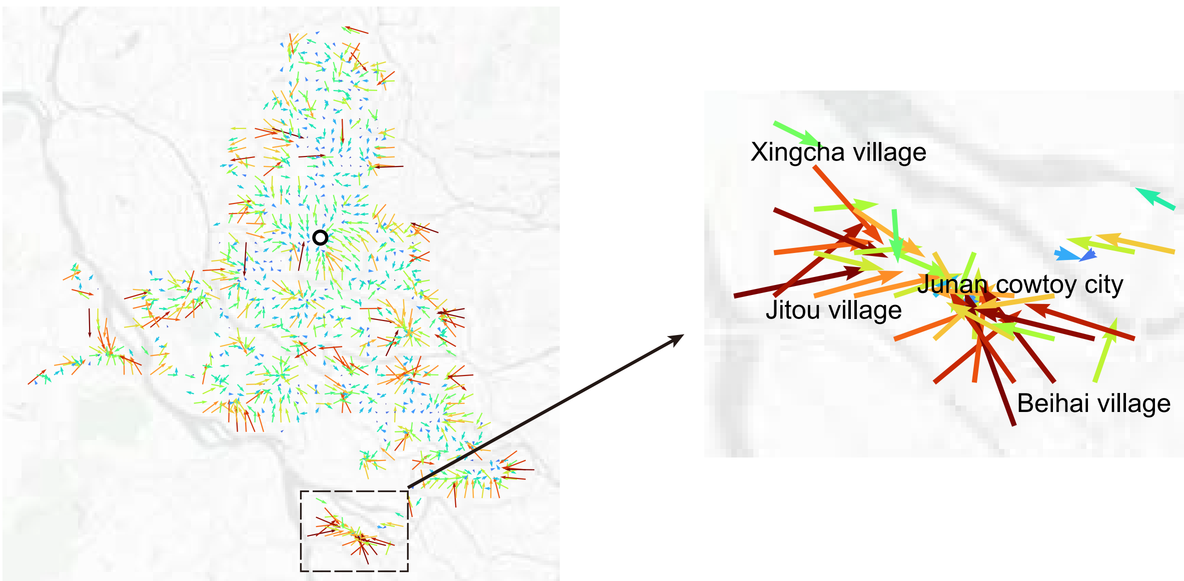

Supplementary Figure 20: **Illustration of the PMV map in Junan.** The left panel displays the PMV map for Foshan and the right panel displays the PMV map for Junan, a town of Foshan. It is evident that the PMVs for Junan are more oriented toward Junan cowtoy city.

Supplementary Table

Supplementary Table 1: **The anisotropy and centripetality of each city.**

City	Λ	Γ	City	Λ	Γ
Beijing	0.397	0.917	Changzhou	0.244	0.743
Shanghai	0.363	0.827	Zhongshan	0.279	0.773
Nanjing	0.359	0.884	Shaoxing	0.311	0.754
Shenzhen	0.33	0.813	Jiaxing	0.267	0.774
Guangzhou	0.363	0.839	Xuzhou	0.35	0.876
Hangzhou	0.36	0.857	Ningbo	0.29	0.853
Chengdu	0.341	0.871	Wenzhou	0.308	0.694
Hefei	0.301	0.821	Wuxi	0.269	0.781
Suzhou	0.277	0.672	Chongqing	0.3	0.856
Jinan	0.359	0.828	Hohhot	0.376	0.931
Wuhan	0.335	0.81	Huizhou	0.312	0.78
Changsha	0.354	0.855	Jiangmen	0.328	0.705
Tianjin	0.28	0.868	Yangzhou	0.328	0.866
Zhengzhou	0.324	0.897	Nantong	0.296	0.859
Harbin	0.356	0.92	Taizhou	0.283	0.821
Shijiazhuang	0.366	0.884	Jinhua	0.343	0.876
Taiyuan	0.401	0.903	Taizhou	0.295	0.748
Shenyang	0.346	0.916	Baoding	0.335	0.902
Lanzhou	0.39	0.854	Handan	0.36	0.926
Xian	0.331	0.881	Xingtai	0.337	0.902
Kunming	0.366	0.902	Cangzhou	0.343	0.91
Guiyang	0.367	0.847	Langfang	0.362	0.914
Nanning	0.326	0.893	Yancheng	0.331	0.88
Dongguan	0.299	0.614	Dalian	0.343	0.83
Foshan	0.303	0.651	Haikou	0.394	0.924
Nanchang	0.322	0.912	Qinhuangdao	0.309	0.861
Xiamen	0.332	0.74	Qingdao	0.283	0.793
Fuzhou	0.407	0.889	Quanzhou	0.343	0.638
Tangshan	0.342	0.861	Yantai	0.3	0.717
Changchun	0304	0.896	Urumqi	0.324	0.867

Supplementary Table 2: **The urban area and population size of each city.**

City	Area(km^2)	Population	City	Area(km^2)	Population
Beijing	2218	17158479	Changzhou	544	2629272
Shanghai	3004	27343905	Zhongshan	209	574342
Nanjing	600	6081413	Shaoxing	354	1503759
Shenzhen	1130	11035114	Jiaxing	196	924229
Guangzhou	1158	12076377	Xuzhou	344	1472710
Hangzhou	1142	5120292	Ningbo	538	2879078
Chengdu	1225	7641941	Wenzhou	612	4523330
Hefei	541	2772965	Wuxi	633	3107485
Suzhou	1149	5050156	Chongqing	448	3782214
Jinan	532	3600159	Hohhot	280	2019896
Wuhan	783	7538878	Huizhou	212	1262870
Changsha	387	3328836	Jiangmen	203	842824
Tianjin	735	7071822	Yangzhou	151	741400
Zhengzhou	596	4942037	Nantong	302	896640
Harbin	518	4329812	Taizhou	118	387496
Shijiazhuang	598	3268020	Jinhua	123	459265
Taiyuan	385	3876707	Taizhou	287	1243473
Shenyang	595	5798014	Baoding	249	1024848
Lanzhou	248	2534533	Handan	173	657165
Xian	563	5127254	Xingtai	130	762290
Kunming	325	3138201	Cangzhou	158	594928
Guiyang	278	2548039	Langfang	116	462727
Nanning	200	1851293	Yancheng	171	407293
Dongguan	1504	4245414	Dalian	586	3532343
Foshan	1261	4463599	Haikou	179	1427056
Nanchang	389	3200554	Qinhuangdao	122	715047
Xiamen	426	2863959	Qingdao	599	3577324
Fuzhou	306	2995036	Quanzhou	961	4224598
Tangshan	382	1491459	Yantai	392	1268417
Changchun	450	3446865	Urumqi	363	3515176

Supplementary Table 3: **The coordinate of the city center identified with MCA.**

City	Longitude	Latitude	City	Longitude	Latitude
Beijing	116.39	39.94	Changzhou	119.96	31.78
Shanghai	121.47	31.22	Zhongshan	113.39	22.52
Nanjing	118.79	32.04	Shaoxing	120.59	30.01
Shenzhen	114.05	22.55	Jiaxing	120.74	30.75
Guangzhou	113.32	23.13	Xuzhou	117.21	34.26
Hangzhou	120.18	30.26	Ningbo	121.58	29.86
Chengdu	104.06	30.64	Wenzhou	120.68	28.00
Hefei	117.26	31.84	Wuxi	120.33	31.55
Suzhou	120.64	31.31	Chongqing	106.54	29.58
Jinan	117.05	36.66	Hohhot	111.70	40.82
Wuhan	114.29	30.59	Huizhou	114.43	23.09
Changsha	113.00	28.18	Jiangmen	113.09	22.59
Tianjin	117.21	39.11	Yangzhou	119.43	32.39
Zhengzhou	113.70	34.77	Nantong	120.89	32.01
Harbin	126.65	45.75	Taizhou	119.93	32.47
Shijiazhuang	114.52	38.04	Jinhua	119.65	29.09
Taiyuan	112.56	37.84	Taizhou	121.43	28.65
Shenyang	123.43	41.79	Baoding	115.49	38.88
Lanzhou	103.84	36.06	Handan	114.51	36.61
Xian	108.94	34.25	Xingtai	114.50	37.07
Kunming	102.73	25.03	Cangzhou	116.85	38.31
Guiyang	106.71	26.58	Langfang	116.72	39.53
Nanning	108.35	22.81	Yancheng	120.16	33.37
Dongguan	113.77	23.01	Dalian	121.62	38.92
Foshan	113.12	23.02	Haikou	110.33	20.02
Nanchang	115.90	28.67	Qinhuangdao	119.59	39.94
Xiamen	118.12	24.5	Qingdao	120.39	36.10
Fuzhou	119.31	26.08	Quanzhou	118.61	24.90
Tangshan	118.18	39.64	Yantai	121.38	37.53
Changchun	125.33	43.88	Urumqi	87.59	43.82

Supplementary Notes

Supplementary Note 1: Illustrating the importance of mobility directionality

Supplementary Fig. 1 presents that a mobility network with the same OD matrix can have multiple distinct layouts, indicating the spatial information has fundamental connections with the overall characteristics of human mobility. To incorporate the spatial information associated with human mobility, we draw inspiration from the route geometric metric [1]. We first vectorize the flow T_{ij} and obtain a vector $T_{ij}\overrightarrow{u_{ij}}$, where $\overrightarrow{u_{ij}}$ is the unit vector from i to j. Then, to factor out the effects of the variation in outflow across locations, we rescale $T_{ij}\overrightarrow{u_{ij}}$ by the outflow of its origin, giving $\overrightarrow{T_{ij}} = T_{ij}\overrightarrow{u_{ij}}/O_i$. Finally, we sum the vectors pointing to all destinations j and obtain the PMV $\overrightarrow{T_i}$, as shown in Fig. 1 in the main text. The PMV inherits the conceptual framework of the route geometric metric, thus unravelling the directional characteristics associated with human mobility. It is worth noting that the PMV coincides mathematically with the vector field for commuting mobility [2]. This coincidence further suggests the rationality of the PMV definition.

Supplementary Note 2: Extracting the urban area

The urban area, an essential spatial property, is widely used in many urban studies such as urban planning and assessment of urban development. However, the definition of urban areas varies with different countries and applications. For example, the conventional method of defining urban areas in the USA is the Metropolitan Statistical Areas, while that in Europe is the Larger Urban Zones [3]. These definitions are inconsistent with one another as no consensus exists on how urban areas should be defined [4]. Note that population is a commonly used indicator for defining human agglomerations. We therefore adopt the global human settlement dataset [5], which defines the urban area as a contiguous area with a density of at least 1500 inhabitants per square kilometer or a majority of buildup land cover coincident with a minimum of 50000 inhabitants, to extract the urban area. Supplementary Fig. 2 depicts the boundary of the urban area (black line) together with the density distribution of outflow per grid in six selected cities. As it can be seen, most of the cells with a large number of outflow are located within the urban area, indicating that the mobile phone dataset and the urban area are highly coincidental.

Supplementary Note 3: Identification results of the city center

The city center identified with the maximum centripetality algorithm is shown in Supplementary Fig. 3, in which each location is colored according to the centripetality Γ of urban mobility when this location is regarded as the city center. The location with the highest centripetality is identified as the city center. It can be seen that the outflow of the surrounding locations of the city center is relatively large, as shown in Supplementary Fig. 4. This is because from the perspective of cost economics, the average travel distance from the city center to other locations is the shortest, which leads to a high proportion of population concentration near the city center, and consequently a large number of outflow. The coordinate of the city center for all 60 cities is listed in Supplementary Table 3. Our algorithm provides an automated and systematic means to identify the city center using human mobility data, thereby eliminating the dependency on subjective definitions or coordinates provided by mapping services. In addition, the city center is defined according to human movements and thus can be viewed as the integrated socioeconomic core of interactions embedded in physical space.

Supplementary Note 4: Classification of cities

We apply the hierarchical clustering method to classify cities based on their similarity (distance) in terms of their anisotropy and centripetality. There are different approaches of hierarchical clustering, such as average linkage, Ward linkage and complete linkage [6].

For the average linkage approach, the distance between two clusters will be calculated as the average distances between all pairs of cities in two clusters. For the Ward linkage approach, it is based on a classical sum-of-squares criterion, producing clusters that minimize the increase in the within-cluster sum of squares at each binary fusion. For the complete linkage approach, the distance between clusters will be calculated as the maximum distance among each pair of cities in two clusters. In the main text, we use the average linkage approach and find that three clusters give the best interpretation (Fig. 2). Additionally, we also use the Ward linkage approach and complete linkage to classify cities (Supplementary Fig. 5) and find that the results are almost the same, suggesting this three-clusters classification is robust and appropriate (Supplementary Fig. 6).

Supplementary Note 5: Spatial distribution of PMVs in different city cluster

In the main paper, we have discussed the mobility characteristics and patterns of various types of cities. Here we further demonstrate the plausibility of our classification and interpretation. Supplementary Figs. 7-9 display representative cities for each of the three types. It can be observed that cities within the same type exhibit similar PMV patterns, while cities of different types exhibit different PMV patterns.

Supplementary Note 6: Spatial hierarchical structure of cities

To factor out the effects of spatial inhomogeneity of population distribution, we model urban space as a hierarchy of l levels according to the principle of equal trip occurrence. If we regard the outflow of the cell as its “mass”, this division of space hierarchy is equivalent to divide the urban space with equal mass. It can be said that this division is a kind of normalization for urban space, establishing a one-to-one corresponding spatial relationship between different cities. In the main text, we use $l = 5$ for all cities, while our results are robust against changes of this value. As shown in Supplementary Fig. 10, there is no quantitative change in our results when varying the number of spatial levels l.

The anisotropy still increases with the spatial level across city types and the centripetality still decreases with the spatial level across city types. Furthermore, despite these regularities are discovered at the city-average level, they are still detected at the single-city level (Supplementary Figs. 11-16), which confirms that the observed regularities are intrinsic and universal properties of urban mobility. It is worth mentioning that the centripetality of all spatial levels in all these cities is greater than 0.5 (Supplementary Figs. 14-16), indicating that, on average, the dominant mobility consistently gravitates towards the urban center (urban core). This result points to the strong influence of urban core, which has an overall attraction effect on all mobility flows in urban area.

On the other hand, for anisotropy, strong monocentric cities still experience the largest increase, followed by weak monocentric cities, and finally polycentric cities (Supplementary Figs. 10a,c). For centripetality, strong monocentric cities still experience the smallest decrease, followed by weak monocentric cities, and finally polycentric cities (Supplementary Figs. 10b,d). These results further confirm the validity of our classification for the three types of cities based on anisotropy and centripetality.

Supplementary Note 7: The anisotropy and centripetality of a spatial level

The anisotropy of a spatial level l ($l = l_1, l_2, l_3, l_4, l_5$) is computed as the weighted average of each location's anisotropy, with the outflow of each location as a weight, i.e.,

$$\Lambda_l = \frac{\sum_{i\in l} O_i \lambda_i}{\sum_{i\in l} O_i}, \tag{1}$$

where Λ_l is the anisotropy of the spatial level l and $i \in l$ denotes i is located in the spatial level l.

In the same way, the centripetality of the spatial level l is computed as the weighted average of each location's centripetality, with the outflow of each location as a weight, i.e.,

$$\Gamma_l = \frac{\sum_{i\in l} O_i \gamma_i}{\sum_{i\in l} O_i}, \tag{2}$$

where $\mathit{\Gamma}_l$ is the anisotropy of the spatial level l and $i \in l$ denotes i is located in the spatial level l.

Supplementary References

[1] Lee, M., Barbosa, H., Youn, H., Holme, P. & Ghoshal, G. Morphology of travel routes and the organization of cities. *Nat. Commun.* **8**, 2229 (2017).

[2] Mazzoli, M. *et al.* Field theory for recurrent mobility. *Nat. Commun.* **10**, 3895 (2019).

[3] Bettencourt, L. M. A. & Lobo, J. Urban scaling in Europe. *J. R. Soc. Interface.* **13**, 20160005 (2016).

[4] Barthelemy, M. The statistical physics of cities. *Nat. Rev. Phys.* **1**, 406–415 (2019).

[5] Florczyk, A. *et al.* GHS-UCDB R2019A—GHS Urban Centre Database 2015, multitemporal and multidimensional attributes. European Commission, Joint Research Centre. https://data.jrc.ec.europa.eu/dataset/53473144-b88c-44bc-b4a3-4583ed1f547e (accessed April 13, 2022)

[6] Govender, P. & Sivakumar, V. Application of k-means and hierarchical clustering techniques for analysis of air pollution: A review (1980–2019). *Atmos. Pollut. Res.* **11**, 40-56 (2020).